



Green Synthesis of Gold Nanoparticles using *Carambola* Fruit Extract and Evaluation of their Antioxidant and Anticancer Efficiency

ALAMPALLY BANGARU BABU^{1,2,✉}, KANAKA DURGA BHAVANI ANAGANI^{1,*✉} and PIDAMARTHI SRAVANTHI^{3,✉}

¹Department of Chemistry, Osmania University, Hyderabad-500007, India

²Department of Chemistry, Government Degree College, Puttur-517583, India

³Department of Chemistry, T.T.W.R. Degree College (M), Maripeda-506315, India

*Corresponding author: E-mail: durgabhavani237@gmail.com

Received: 20 November 2022;

Accepted: 18 February 2023;

Published online: 27 February 2023;

AJC-21170

In this study, a successful synthesis of gold nanoparticles (AuNPs) using extract from the *Carambola* fruit was carried out. Remarkably fast reduction of Au³⁺ ions was observed when aqueous chloroauric acid was treated with star fruit powder at 60 °C and this was obtained without the use of any stabilizing or reducing agents. The UV-visible, FT-IR, DLS, XRD, SEM and TEM were used to study the synthesized AuNPs. The FT-IR studies suggested that the phenolic group may have contributed to the reduction of Au³⁺. The DLS particle size analysis and TEM measurements revealed that AuNPs had a mean particle size of 10 nm and were nearly spherical in form. The crystalline character of AuNPs was established by TEM-SAED image and XRD analyses. Zeta potential measurements were used to analyze the stability of AuNPs. The synthesized AuNPs effectively scavenge free radicals such as DPPH, NO^{*} and H₂O₂ with % inhibition values of 57.12, 58.75 and 60.23, respectively. The MTT assay of the anticancer activity demonstrated that the synthesized AuNPs worked effectively against MCF7 cell lines and are comparable to those of standard cancer drugs.

Keywords: Gold nanoparticles, *Carambola* fruit extract, Antioxidant activity, Anticancer activity.

INTRODUCTION

Nanotechnology studies include controlled monodispersity nanoparticles of various forms, sizes and chemical compositions [1]. Due to their use in catalysis, drug delivery, medicines, biotechnology, cancer therapy and electronics, metal based nanoparticles have garnered wide research interest [2]. Metal nanoparticles also regulate air and water pollution [3]. They are effective antibacterial agents whether synthesized chemically [4,5] or from plant extracts [6]. Gold nanoparticles (AuNPs) are biocompatible and used in cancer diagnosis, photothermal therapy and drug delivery [7] and also found to be least hazardous metal nanoparticles to animals and microbes [2].

There are several methods for synthesizing nanoparticles; e.g. physical, chemical and biological methods. Chemical procedures involve several organic solvents and toxic chemicals, restricting their medical applicability and producing hazardous wastes [8]. Synthesis of green metal nanoparticles approach seems to be promising and high sustainable therapeutic efficacy,

tailored binding, low toxicity and site-specific administration [9-11]. Plants like *Capsicum Chinense*, *Jatropha integerrima* Jacq., *Curcuma pseudomontana*, *Vitex negundo*, Onion peel, *Sumac*, Lavender, *Citrullus lanatus*, *Bauhinia purpurea*, Gum arabic, etc. [12-22] have been used for the synthesis of AuNPs and characterized. The promising bioactive components present in the aqueous extracts of these plants are responsible for the conversion of Au³⁺ ions into AuNPs.

Few metal nanoparticles viz. CuO, ZnO and MgO nanoparticles are already synthesized from the aqueous extract of star fruit [23]. According to the studies [24], *Carambola* fruits are an excellent source of common antioxidants like carotene, magnesium, potassium and phosphorous. Star fruits also contain antioxidants including iron, zinc and manganese, which support a stronger immune system. The objective of the current investigation is to synthesize AuNPs from the aqueous extract of star fruit. Several spectral and microscopic techniques, including UV-visible, FT-IR, DLS, XRD, SEM and TEM, are used to characterize the synthesized gold nanoparticles. In addition,

the antioxidant and anticancer (against breast cancer cells) properties of the synthesized AuNPs were also evaluated.

EXPERIMENTAL

The ripened *Carambola* fruits were purchased from the local fruit market of Hyderabad city, India. All of the chemicals used were of analytical reagent grade and did not require further purification. All the experiments were conducted with Milli-Q water.

Biosynthesis gold nanoparticles using *Carambola* (star) fruit extract: Ripened *Carambola* (star) fruits were cleaned with milli-Q water and allowed to dry in the sun for ten days to remove moisture. The dried fruit was cut and finely powdered in the electric mixer. Accurately weighed 1 g and 2 g of star fruit powder was added to 10 mL of Milli-Q water separately followed by addition of 10 mL of 1.67×10^{-3} M aqueous HAuCl₄ solution in 250 mL Erlenmeyer flasks. The flasks were then placed in a water bath heated to 60 °C. A pale-yellow solution became purple within 5 min, suggesting the formation of AuNPs. Periodically, a nanodrop spectrophotometer recorded the production of gold nanoparticles.

Characterization: The UV-visible spectra of the prepared nanomaterial solution were recorded by a Shimadzu spectrophotometer (UV-1650 PC) in the wavelength range from 200–800 nm at room temperature. The sample was scanned between 4000 and 500 cm⁻¹ using an FT-IR spectrometer (Bruker, Germany). The crystalline nature, crystal structure and average particle size of the synthesized gold nanoparticles were determined by using Rigaku Tokyo X-ray Diffractometer using Cu K α 1 radiation ($\lambda = 1.5406 \text{ \AA}$) and a filter of nickel at 40 kV. Horiba nano Partica Analyser (SZ100) Dynamic Light Scattering (DLS) method was used to determine the average particle size in solution and zeta potential of synthesized nanoparticles. A Jeol 639 OLA/Oxford XMXN model Electron Microscope was used to acquire a SEM picture and electron diffraction spectrum (EDX) of the sample. The Jeol/JEM2100 was used to obtain the HR-TEM micrographs.

DPPH radical scavenging activity: A method proposed by Blois [25] was used to assess the radical scavenging capacity of the nanoparticles with DPPH radical. A control reading of the absorbance at 517 nm was immediately taken after the addition of 1 mL of DPPH solution to 3 mL of methanol. For every 4 mL of 0.004% (w/v) methanolic DPPH solution, 1 mL of different concentrations of nanoparticle compounds (25 to 100 $\mu\text{g/mL}$) and the reference component (ascorbic acid) were added. Using methanol as blank, the UV-visible spectrometer was used to measure the absorbance at 517 nm after 30 min of room temperature incubation. For both standard sample and each test compound, the IC₅₀ values were determined. Eqn. 1 was used to determine the free radical scavenging activity of synthesized AuNPs against DPPH.

$$I (\%) = \frac{A_{\text{control}} - A_{\text{sample}}}{A_{\text{control}}} \times 100 \quad (1)$$

where A_{sample} is the absorbance of test sample and A_{control} is an absorbance of control.

Nitric oxide (NO) scavenging activity: In this work, a reported approach [26] was used to assess the nitric oxide scavenging activity. In brief, sodium nitroprusside (10 mM) and phosphate buffer saline (0.2 M, pH 7.4) were added to 1 mL of the test compounds at various concentrations and the mixture was incubated at 25 °C 120 min before being treated with 1 mL of Griess reagent. At 546 nm, the chromophore's absorbance was determined. The prevention of nitric oxide generation in comparison to standard ascorbic acid was measured. The free radical scavenging activity of the synthesized AuNPs against NO was determined using eqn. 1.

Hydrogen peroxide (H₂O₂) scavenging activity: In phosphate buffer, a 40 mM H₂O₂ solution was prepared (pH 7.4). A solution of H₂O₂ (0.6 mL, 40 mM) and phosphate buffer (3.4 mL) were mixed with the various concentrations of gold nanoparticles and ascorbic acid (25, 50, 75 and 100 $\mu\text{g/mL}$). After 5 min of incubation, this reaction mixture OD value measured at 230 nm, the absorbance (OD) value of reaction mixture was measured using phosphate buffer as blank [27]. The free radical scavenging capacity of AuNPs against H₂O₂ was also calculated using eqn. 1.

Anticancer activity: The MTT assay [28] was used to measure cell viability in using triplicate with gold nanoparticles at five different doses. Cells in suspension were trypsinized and subjected to the trypan blue assay to measure their viability. Cells were counted using a hemacytometer and plated at a density of 5×10^3 cells per well in 100 μL of culture media in 96-well plates for an overnight incubation at 37 °C. After incubation, added the fresh media containing 100 μL of test compound at various concentrations in the corresponding wells of 96-plates. After 48 h, remove the drug solution and replace it with fresh drug containing MTT solution (0.5 mg/mL). The plates then incubated for 3 h at 37 °C. At the end of the incubation time, the precipitates were formed when cells with metabolically active mitochondria convert the MTT salt to chromophore formazan crystals. The optical density of dissolved crystals was measured at 570 nm on a microplate reader. The percentage growth inhibition was calculated using the following formula:

$$\text{Inhibition (\%)} = \frac{100 (\text{Control} - \text{Treatment})}{\text{Control}}$$

The IC₅₀ value was calculated using the linear regression equation ($y = mx + c$).

RESULTS AND DISCUSSION

The star fruit powder consists of elements such as vitamin-C (ascorbic acid), gallic acid and tartaric acid with hydroxyl and carboxylic groups and is ideal for the systemic production of colloidal gold nanoparticles from the aqueous solution of aurochloric acid. After 5 min, all Au³⁺ ions had been reduced. Biological components in star fruit powder extract served as capping and reducing agents, converting Au³⁺ in the solution into Au⁰ nanoparticles (Fig. 1).

Two different quantities of star fruit powder (1 and 2 g) were examined while maintaining 10 mL of aurochloric acid, and it was determined that the reaction mixture containing 1 g

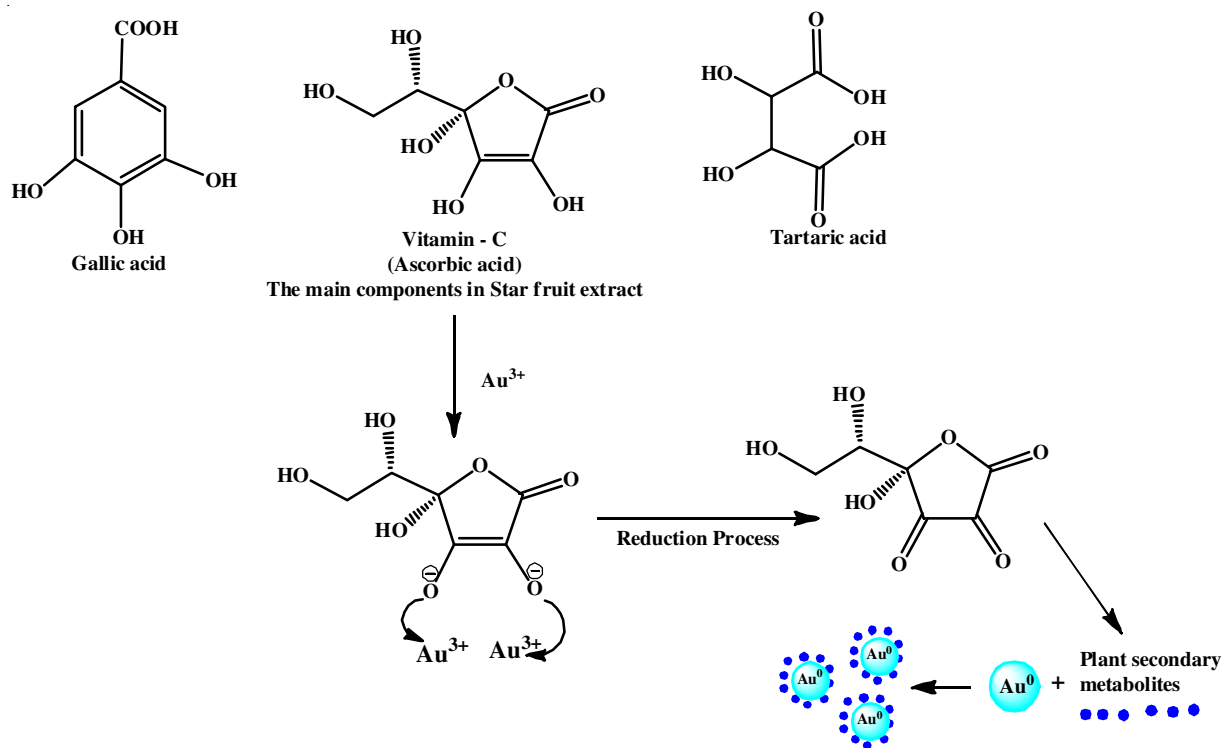


Fig. 1. Proposed mechanism for reducing AuNPs by Star fruit powder

of star fruit powder exhibited the highest intensity peak at 545 nm (Fig. 2). Whereas absorbance was found to be decreased in case of the reaction mixture containing 2 g star fruit powder which is possible due to the agglomeration of nanoparticles in the colloidal solution.

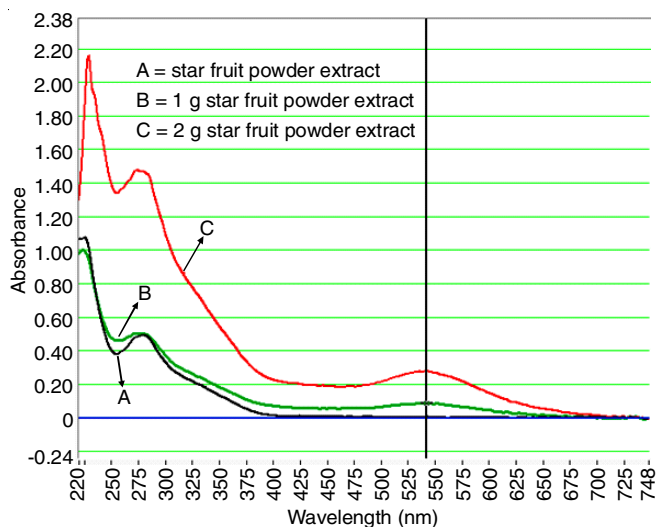


Fig. 2. UV-visible spectrum of the synthesized star fruit extract mediated AuNPs

UV-visible studies: The UV-visible spectrum of the green synthesized AuNPs is shown in Fig. 2. According to the spectral investigation, AuNPs have a unique absorption peak at 545 nm with a high absorption value [14,19,20]. In this region, no peak was found for the star fruit powder extract. This proved that the phytochemicals present in the star fruit powder served

as capping and stabilizing agents during the synthesis of nanoparticles.

FT-IR studies: The star fruit powder extract and colloidal AuNPs were analyzed by FT-IR to determine the role of reducing ability of star fruit extract. The FT-IR peaks of star fruit powder extract were appeared at 3897-3278, 2924, 1723, 1244, 972 and 567 cm^{-1} (Fig. 3a), whereas the FT-IR spectral peaks of AuNPs were observed at 3320 and 1637 cm^{-1} (Fig. 3b). A peak at 3278 cm^{-1} is due to the hydroxyl group (-OH) stretching frequency of star fruit powder extract, which have shifted to 3320 cm^{-1} in AuNPs. This vibration corresponds to the hydroxyl function in alcohol or phenolic compounds present in star fruit extract. A peak at 1723 cm^{-1} in star fruit extract was due to the carboxylic group and this stretching frequency was shifted to 1637 cm^{-1} AuNPs because of the presence of biomolecules in the star fruit powder extract. It has been suggested that the biomolecules in star fruit extract converted the Au^{3+} into Au^0 nanoparticles through phenolic groups.

XRD studies: Five prominent peaks at $2\theta = 38.46^\circ$, 44.69° , 64.79° and 78.00° correspond to the (111), (200), (220) and (311) miller planes, were identified by the XRD pattern (Table-1). When comparing JCPDS card No. 04-0784 to XRD data, it is evident that the peaks reflect the face centered cubic (FCC) phase of gold nanoparticles (Fig. 4). In addition, the XRD patterns reveal no other diffraction peaks associated with the contaminants and no significant shift in any diffraction peaks, indicating the purity of the synthesised gold nanoparticles. These findings were in good accord with AuNPs that had previously been described [16,20].

Utilizing the Debye-Scherrer's equation, the crystallite size (nm) was determined using following equation:

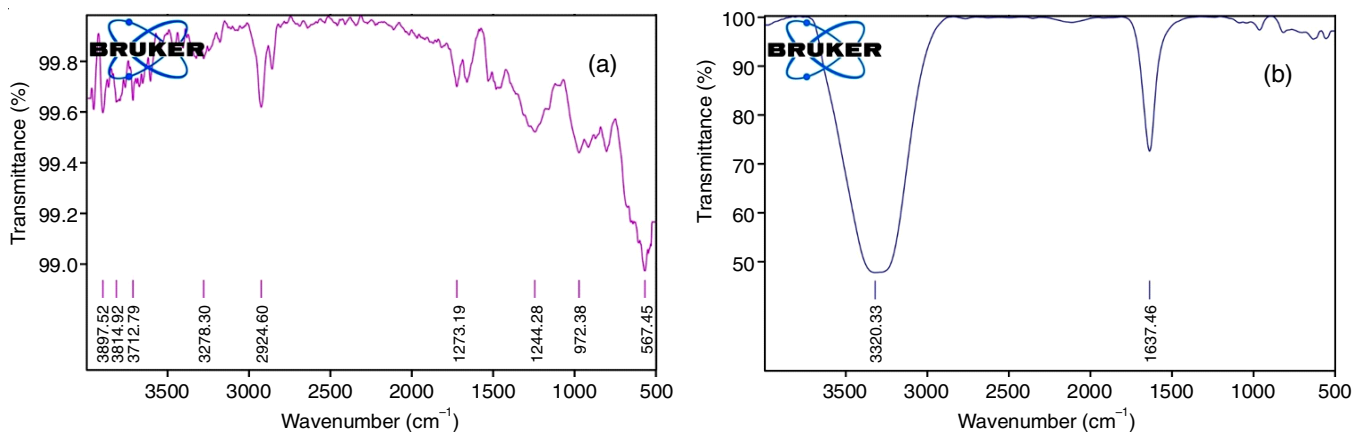


Fig. 3. (a) FT-IR spectrum of star fruit extract and (b) synthesized AuNPS

S. No.	d-spacing (Å) Standard JCPDS No: 04-0783	Intensity	2θ values from XRD spectrum	Calculated d-spacing (Å)	(h k l)
1	2.355	100	38.46	2.338771	111
2	2.039	52	44.69	2.026131	200
3	1.422	32	64.79	1.437789	220
4	1.230	36	78.00	1.224019	311

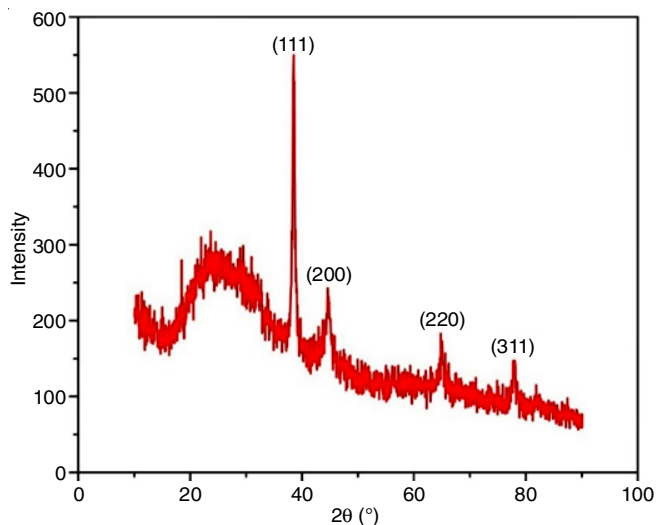


Fig. 4. XRD spectrum of AuNPs prepared by star fruit extract

$$D = \frac{0.94\lambda}{\beta \cos \theta}$$

where λ is the X-ray wavelength, D is the average crystallite size and β is the width at half maximum, θ is the Bragg angle. The calculated average crystallite size was found to be 20 nm.

Dynamic light scattering (DLS) studies: Fig. 5a-b illustrates the size distribution and zeta potential of the synthesized AuNPs through the dynamic light scattering method (DLS). The hydrodynamic size of the AuNPs was ranged between 1 to 10 nm. The synthesized colloidal gold nanoparticles have a zeta potential of -12.4 mV, which is negative and indicating of the strong surface electric charge of the nanoparticles. The biomolecules with a negative charge on the nanoparticles surface were the reason of this negative zeta potential and results in the efficient stabilization of AuNPs. The DLS measurement size is often not as those measured by TEM. Therefore, the size

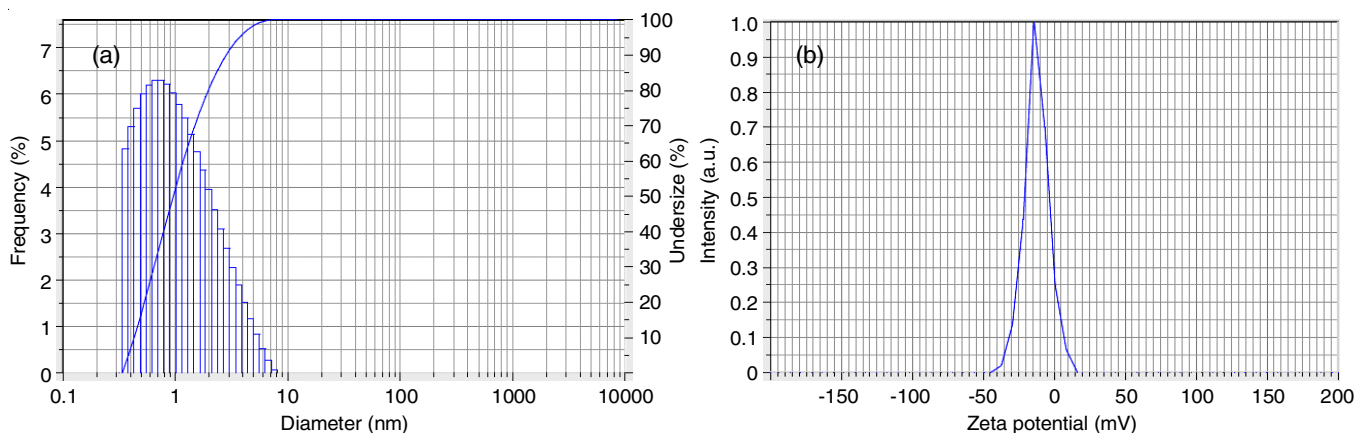


Fig. 5. (a) Particle size distribution curve and (b) Zeta potentials of the synthesized star fruit extract mediated AuNPs

difference between TEM and DLS could be due to the sampling volume used during the analysis.

Morphological studies: The biological reduction of Au³⁺ into AuNPs was verified by EDX. Green synthesized AuNPs in Fig. 6a reveal a clear signal at 2.2, 9.5, 10.3, 11.5 and 13.4 keV, the same values as elemental gold. The spectral signals of the other elements C, O and K also appeared as a result of the elements present in the star fruit extract. A copper peak was also observed, which may have come from the carbon coated copper grid used in the study.

Fig. 6b shows the SEM micrographs of green synthesized AuNPs using star fruit extract. SEM micrographs confirmed that the metal particles were mono-size with a spherical shape and uniformly distributed. SEM images taken one month after synthesis revealed that the nanoparticles had not aggregated, and thus indicating their stability. The particle size was found to be between 40 and 80 nm by analyzing SEM micrographs with the ImageJ software.

TEM and SAED studies: The spherical shape particles were observed under TEM, which was very small indicating that star fruit extract-mediated AuNPs are more effective in cytotoxic, antioxidant, antimicrobial and catalytic applications. The mean particle size of the gold nanoparticles shown in Fig. 7a-b was found to be between 10 to 20 nm. The calculated inter-planar distance of about 0.24 nm is represented in Fig. 7c.

In addition, the crystalline structure of star fruit extract mediated AuNPs was determined using the pattern of selected area electron diffraction (SAED) (Fig. 7d). The brilliant circles correlate to the polycrystallinity of the nanoparticles of gold. The circular rings assigned to (111), (200), (220) and (222) observed in the SAED pattern are the characteristic reflections of FCC crystalline structure. The results of the SAED and XRD analysis were consistent with one another.

Antioxidant activities: Three different assays *viz.* DPPH radical scavenging assay, nitric oxide (NO) and hydrogen peroxide (H₂O₂) scavenging assays were used to assayed the antioxidant capacity of the synthesized AuNPs. As indicated in Table-2, all the samples exhibit the strong free radical scavenging activity.

DPPH Scavenging activity: The DPPH method was used to evaluate the antioxidant effectiveness of green-synthesized AuNPs prepared from star fruit extract (Fig. 8). The colour of the solution changed from purple to light yellow as it was exposed to gold nanoparticles. Specifically, an absorption peak at 517 nm suggested that the synthesized gold nanoparticles from star fruit have antioxidant properties. According to the findings, the effectiveness of gold nanoparticles and the gold standard chemical, ascorbic acid, varied with their concentrations. At 100 µg/mL, the IC₅₀ values for AuNPs and ascorbic acid were 77.22 and 52.92, respectively, indicating 57.12% and 78.36% of the scavenging activity. The ability of gold nanoparticles to scavenge DPPH radicals may be explained by their ability to transfer electrons or hydrogen ions to DPPH radicals, leaving them inactive. Studies have shown that antioxidant activity of the prepared AuNPs *via* green synthesis is higher than that of AuNPs prepared using conventional chemical techniques [29].

Nitric oxide scavenging activity: Fig. 9 displays the scavenging ability of the synthesized AuNPs against nitric oxide (NO). The synthesized AuNPs were taken in different concentrations ranging from 25-100 µg/mL. The results showed that at 100 µg/mL of AuNPs derived from star fruit extract had a maximum scavenging activity of 51.20%, however, possessed lower nitric oxide scavenging activity than the reference compound ascorbic acid (63.40%) at 100 µg/mL. According to Fig. 9, the IC₅₀ value for AuNPs and ascorbic acid was determined to be 73.15 µg/mL and 77.63 µg/mL, respectively. The major phytochemicals contained in star fruit extracts serve as a capping agent and were primarily responsible for the antioxidant activity of AuNPs.

H₂O₂ scavenging activity: The H₂O₂ experiment was performed with different concentrations ranging from 25-100 µg/mL and the results indicate that increasing the concentration of AuNPs enhances the radical scavenging activity and shows the highest scavenging activity of 60.75% for 100 µg/mL with a (IC₅₀) value of 84.59 µg/mL. However, it uses the same amount of ascorbic acid and has 79.38% H₂O₂ scavenging activity with an IC₅₀ value of 50.52 µg/mL (Fig. 10). Hydrogen peroxide is

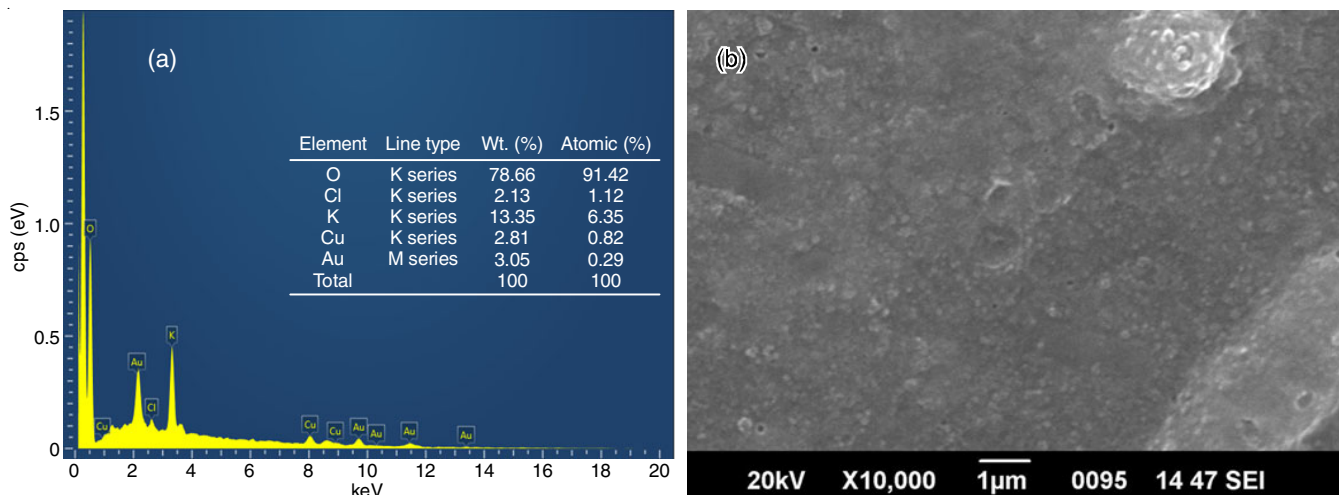


Fig. 6. (a) EDX spectrum and (b) Scanning electron microscope image of star fruit extract mediated AuNPs

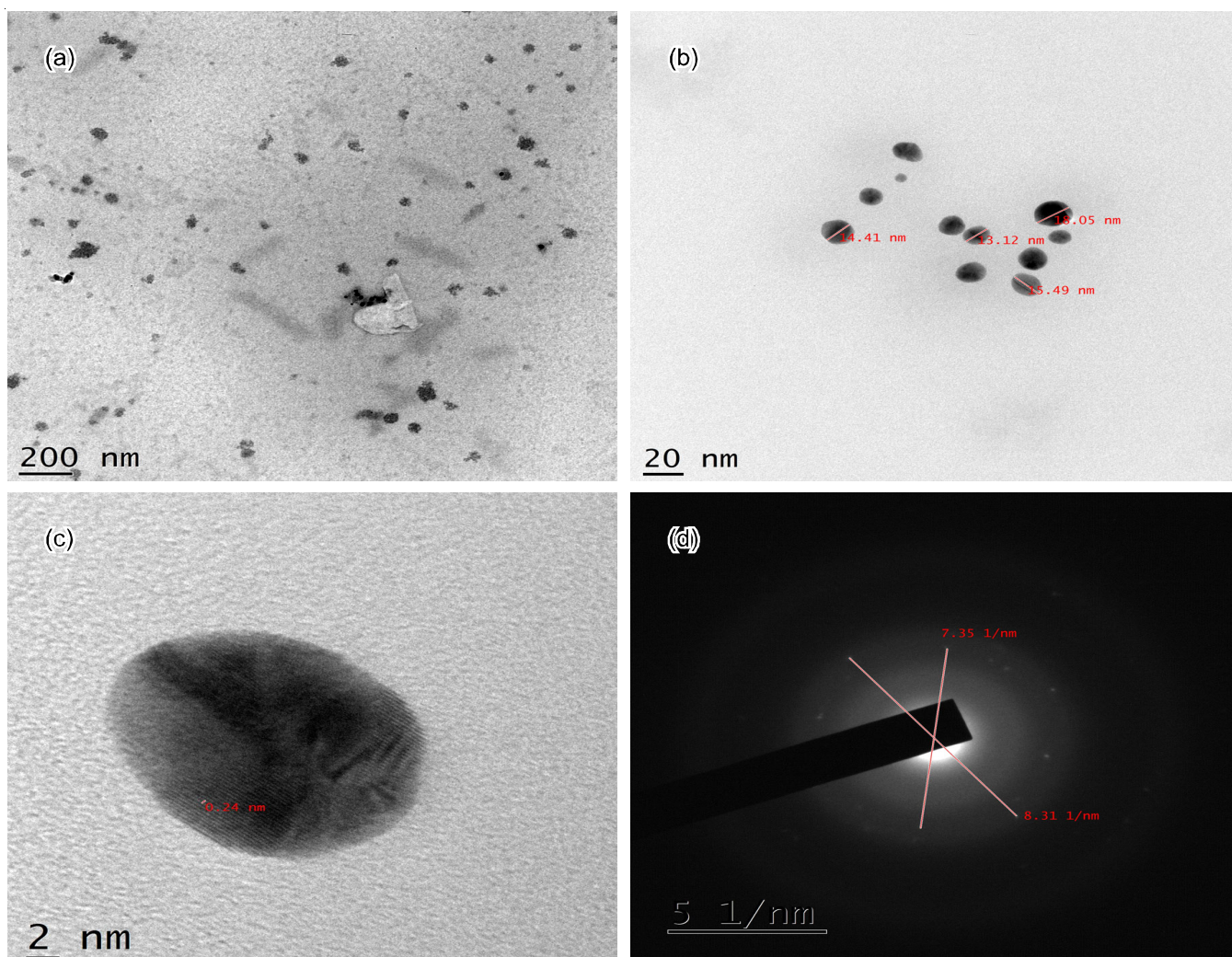


Fig. 7. (a-b) Transmission electron microscope images, (c) Interplanar distance and (d) SAED pattern of star fruit extract mediated AuNPs

TABLE-2
ANTIOXIDANT ACTIVITY OF SYNTHESIZED AuNPs AND ASCORBIC ACID (STANDARD)
SHOWING PERCENTAGE OF INHIBITION AND IC₅₀ VALUES USING DPPH, NO AND H₂O₂ ASSAYS

Assay	Sample	25 µg/mL	50 µg/mL	75 µg/mL	100 µg/mL	IC ₅₀ µg/mL
DPPH	Synthesized AuNPs	36.40 ± 2.75	40.40 ± 3.10	48.56 ± 3.40	57.12 ± 3.20	77.22
	Ascorbic acid (Standard)	34.18 ± 2.50	47.24 ± 3.40	58.40 ± 2.60	78.36 ± 3.20	52.92
NO	Synthesized AuNPs	37.14 ± 1.25	45.72 ± 2.83	51.26 ± 2.77	58.75 ± 2.39	73.15
	Ascorbic acid (Standard)	37.40 ± 2.58	48.82 ± 2.30	63.40 ± 2.72	85.30 ± 2.88	51.20
H ₂ O ₂	Synthesized AuNPs	31.60 ± 2.15	47.60 ± 3.20	55.44 ± 2.40	60.23 ± 2.60	52.52
	Ascorbic acid (Standard)	39.20 ± 2.15	49.48 ± 2.60	65.40 ± 2.60	79.38 ± 3.20	50.52

not a good reactive, but it can be toxic to cells since it produces the hydroxyl radicals.

Anticancer activity: Because of their unique properties, AuNPs are used in the diagnosis and treatment of human cancer. They are safe for healthy cells and do not negatively affect the human body. On the MCF7 cell line, a dose-dependent cytotoxicity experiment of the synthesized AuNPs was performed and for the cell viability experiments, MTT colourimetric assay method was used.

Fig. 11a shows the percentage of the cancer cell line deaths caused by the drug treatment; this data was collected using the MTT assay. As a cancer treatment, the synthesized AuNPs

performed exceptionally well (Table-3). At 5, 10, 25, 50 and 100 µg/mL, the cytotoxic effect of AuNPs against the breast cancer cell line was 7.37%, 18.14%, 36.67%, 53.33% and 66.67%, respectively (Fig. 11b). The IC₅₀ values for AuNPs against the cancer cell were 60.36 µg/mL. The antioxidants present in the star fruit extract may account for the anticancer properties of the AuNPs.

Conclusion

In this work, the gold nanoparticles were synthesized by reducing a gold precursor solution with an extract of *Carambola* fruit also known as star fruit at 60 °C. The synthesis process is

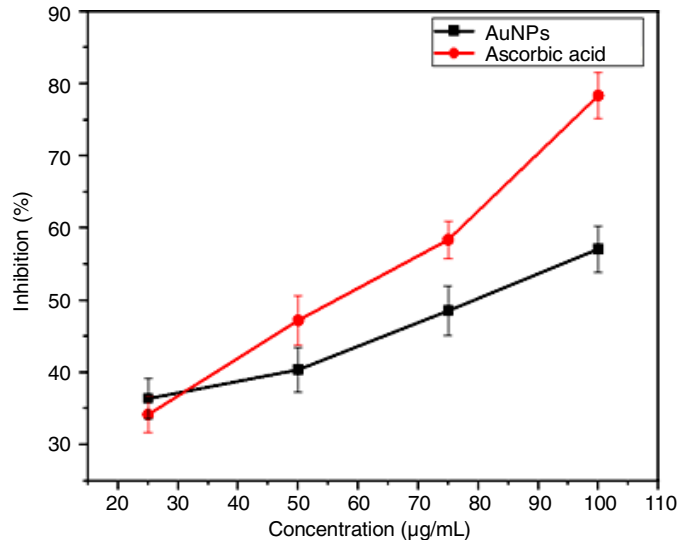
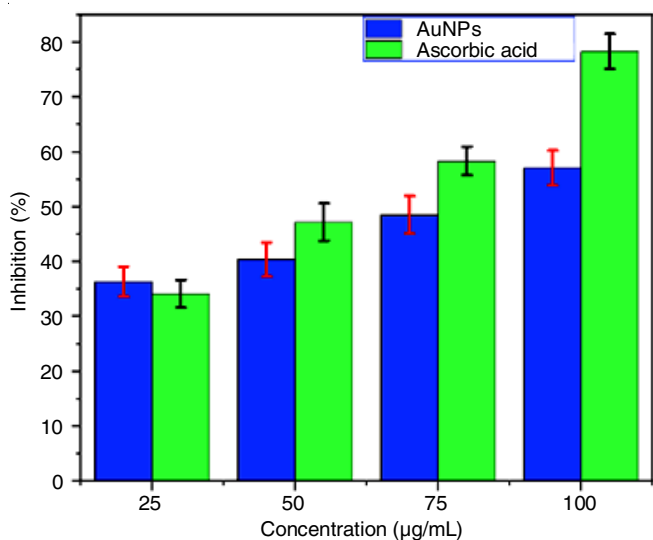


Fig. 8. DPPH radical scavenging activity of star fruit extract mediated AuNPs by green method

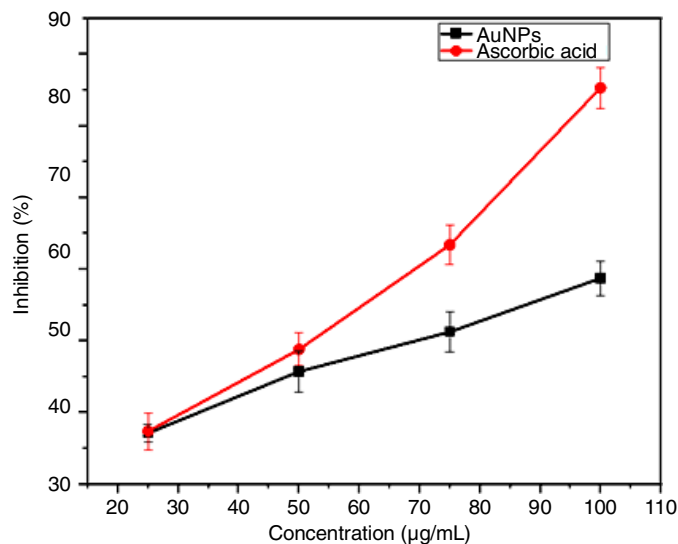
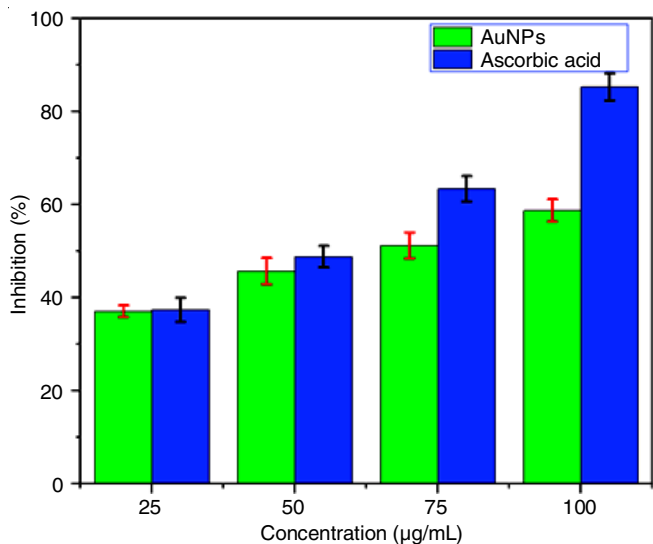


Fig. 9. Nitric oxide scavenging activity of star fruit extract mediated AuNPs

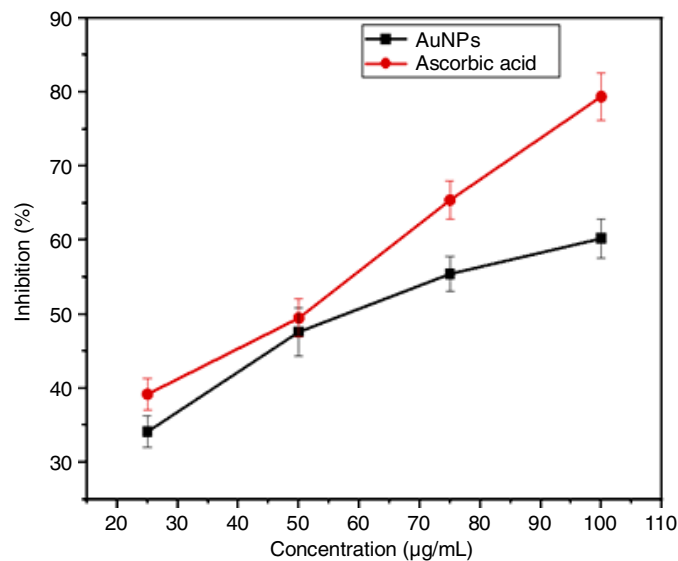
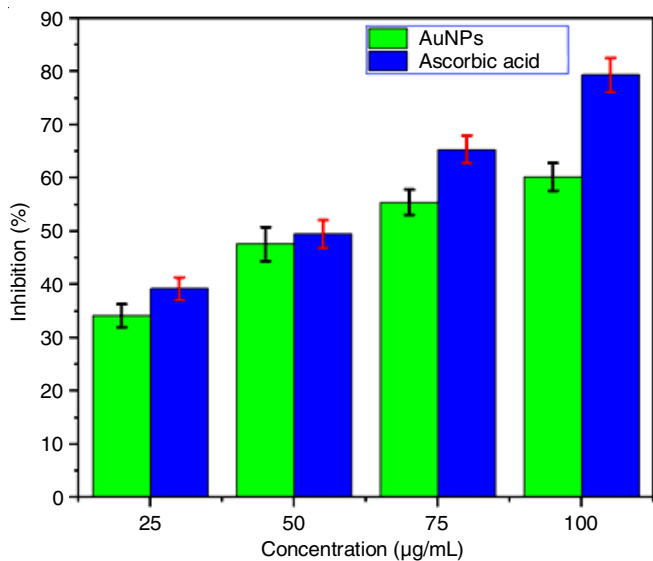


Fig. 10. Hydrogen peroxide radical scavenging activity of star fruit extract mediated AuNPs

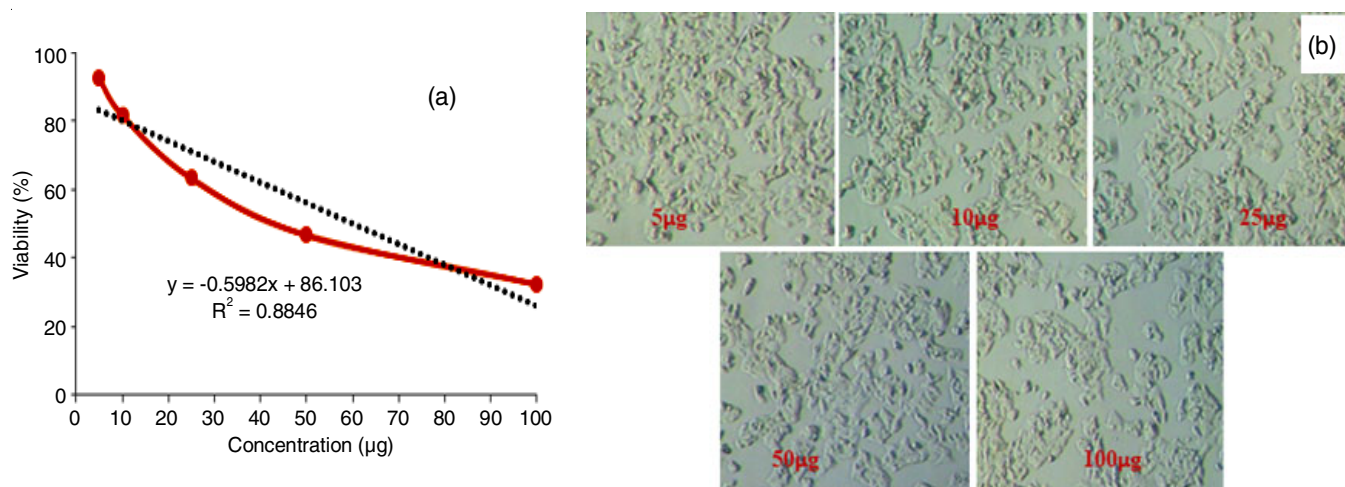


Fig. 11. (a) *In vitro* cell viability assay of synthesized AuNPs on MCF7 cell line. Cells were treated with the AuNPs for 48 h at 36 °C cell viability was measured by the MTT method and (b) Photographic images of MCF 7 cell line treated with 5 µg to 100 µg AuNPs

TABLE-3
DOSE DEPENDENT CELL VIABILITY
STUDIES OF SYNTHESIZED AuNPs BY MTT
ASSAY ON THE MCF7 CELL LINE AT 48 h

Conc. (µg)	Absorbance at 570 nm	Inhibition (%)	Viability (%)	IC ₅₀ (µg)
5	0.490	7.37	92.63	60.36
10	0.433	18.14	81.86	
25	0.335	36.67	63.33	
50	0.247	53.30	46.70	
100	0.171	67.67	32.33	
Untreated	0.529	0	100	
Blank	0	0	0	

ecologically benign and energy efficient since it requires neither stirring nor pH adjustment. The average particle size of AuNPs, which ranges from 1 to 10 nm, was determined using DLS, FE-SEM and HR-TEM investigations. In terms of their potential for use in biological applications, the synthesized AuNPs were stable and well-capped. The green synthesized gold nanoparticles exhibit an excellent antioxidant activity of about 50% in effectively scavenging DPPH, NO and H₂O₂ radicals with IC₅₀ values of 77.22 µg/mL, 73.15 µg/mL and 52.52 µg/mL, respectively. Moreover, AuNPs have demonstrated the highest anticancer activity against human breast cancer cells (MCF7), with IC₅₀ values of 60.36 µg/mL. Based on these findings, it appears that the multifunctional synthesized gold nanoparticles may be used in various biological applications.

ACKNOWLEDGEMENTS

The authors are thankful to Dr. Y. Subba Rao, DST-PURSE Centre, Sri Venkateswara University, Tirupati, India for providing the instrumentation facilities. The authors are also thankful to DST-SAIF Cochin for the SEM & TEM analysis.

CONFLICT OF INTEREST

The authors declare that there is no conflict of interests regarding the publication of this article.

REFERENCES

- M.P. Patil, M. Kang, I. Niyonizigiye, A. Singh, J.-O. Kim, Y.B. Seo and G.-D. Kim, *Colloids Surf. B Biointerfaces*, **183**, 110455 (2019); <https://doi.org/10.1016/j.colsurfb.2019.110455>
- C. Barai, K. Paul, A. Dey, S. Manna, S. Roy, C. Mukhopadhyay and B.G. Bag, *Nano Conver.*, **5**, 10 (2018); <https://doi.org/10.1186/s40580-018-0142-5>
- S. Mditana, S.R. Tirukkavalluri and I.M. Raju, *Nano Systems: Phys. Chem. Maths*, **13**, 104 (2022); <https://doi.org/10.17586/2220-8054-2022-13-1-104-114>
- O.M. El-Borady, M.S. Ayat, M.A. Shabrawy and P. Millet, *Adv. Powder Technol.*, **31**, 4390 (2020); <https://doi.org/10.1016/j.apt.2020.09.017>
- E. Darabpour, N. Kashef, S.M. Amini, S. Kharrazi and G.E. Djavid, *J. Drug Deliv. Sci. Technol.*, **37**, 134 (2017); <https://doi.org/10.1016/j.jddst.2016.12.007>
- A.I. El-Batel, A.A.M. Ashem and N.M. Abdelbaky, *Sringerplus*, **2**, 129 (2013); <https://doi.org/10.1186/2193-1801-2-129>
- M.S. Kang, S.Y. Lee, K.S. Kim and D.-W. Han, *Pharmaceutics*, **12**, 701 (2020); <https://doi.org/10.3390/pharmaceutics12080701>
- K.K. Bharadwaj, B. Rabha, S. Pati, T. Sarkar, B.K. Choudhury, A. Barman, D. Bhattacharjya, A. Srivastava, D. Baishya, H.A. Edinur, Z. Abdul Kari and N.H. Mohd Noor, *Molecules*, **26**, 6389 (2021); <https://doi.org/10.3390/molecules26216389>
- M. Hassanisaadi, G.H. Bonjar, A. Rahdar, S. Pandey, A. Hosseinipour and R. Abdolshahi, *Nanomaterials*, **11**, 2033 (2021); <https://doi.org/10.3390/nano11082033>
- K. Perveen, F.M. Husain, F.A. Qais, A. Khan, S. Razak, T. Afsar, P. Alam, A.M. Almajwal and M.M.A. Abulmeaty, *Biomolecules*, **11**, 197 (2021); <https://doi.org/10.3390/biom11020197>
- B. Rabha, K.K. Bharadwaj, N. Boro, A. Ghosh, S.K. Gogoi, R.S. Varma and D. Baishya, *Green Chem.*, **23**, 7701 (2021); <https://doi.org/10.1039/D1GC02260A>
- D.A. Lomeli-Rosales, A. Zamudio-Ojeda, O.K. Reyes-Maldonado, M.E. López-Reyes, G.C. Basulto-Padilla, E.J. Lopez-Naranjo, V.M. Zuñiga-Mayo and G. Velázquez-Juárez, *Molecules*, **27**, 1692 (2022); <https://doi.org/10.3390/molecules27051692>
- G. Suriyakala, S. Sathiyaraj, R. Babujanathanam, K.M. Alarjani, D.S. Hussein, R.A. Rasheed and K. Kanimozhi, *J. King Saud Univ. Sci.*, **34**, 101830 (2022); <https://doi.org/10.1016/j.jksus.2022.101830>
- N. Muniyappan, M. Pandeewaran and A. Amalraj, *Environ. Chem. Ecotoxicol.*, **3**, 117 (2021); <https://doi.org/10.1016/j.enceco.2021.01.002>

15. S. Veena, T. Devasena, S.S.M. Sathak, M. Yasasve and L.A. Vishal, *J. Cluster Sci.*, **30**, 1591 (2019); <https://doi.org/10.1007/s10876-019-01601-z>
16. H. Shabestarian, M. Homayouni-Tabrizi, M. Soltani, F. Namvar, S. Azizi, R. Mohamad and H. Shabestarian, *Mater. Res.*, **20**, 264 (2017); <https://doi.org/10.1590/1980-5373-mr-2015-0694>
17. B. Kumar, K. Smita, K.S. Vizuete and L. Cumbal, *Biol. Med.*, **8**, 290 (2016); <https://doi.org/10.4172/0974-8369.1000290>
18. J.K. Patra, Y. Kwon and K.-H. Baek, *Adv. Powder Technol.*, **27**, 2204 (2016).
19. J.K. Patra and K.-H. Baek, *Int. J. Nanomedicine*, **10**, 7253 (2015); <https://doi.org/10.2147/IJN.S95483>
20. R. Vijayan, S. Joseph and B. Mathew, *Bioprocess Biosyst. Eng.*, **42**, 305 (2019); <https://doi.org/10.1007/s00449-018-2035-8>
21. E. Mzwd, N.M. Ahmed, N. Suradi, S.K. Alsaee, A.S. Altowyan, M.A. Almessiere and A.F. Omar, *Sci. Rep.*, **12**, 10549 (2022); <https://doi.org/10.1038/s41598-022-14339-y>
22. P. Kumari and A. Meena, *Colloids Surf. A Physicochem. Eng. Asp.*, **606**, 125447 (2020); <https://doi.org/10.1016/j.colsurfa.2020.125447>
23. S. Suresh, S. Vennila, J.A. Lett, I. Fatimah, F. Mohammad, H.A. Al-Lohedan, S.F. Alshahateet, M.A.M. Hossain and M.R. Johan, *Inorg. Nano-Met. Chem.*, **52**, 173 (2022); <https://doi.org/10.1080/24701556.2021.1880437>
24. N. Muthu, S.Y. Lee, K.K. Phua and S.J. Bhore, *Bioinformation*, **12**, 420 (2016); <https://doi.org/10.6026/97320630012420>
25. X.-J. Duan, W.-W. Zhang, X.-M. Li and B.-G. Wang, *Food Chem.*, **95**, 37 (2006); <https://doi.org/10.1016/j.foodchem.2004.12.015>
26. L. Marcocci, L. Packer, M.T. Droy-Lefaix, A. Sekaki and M. Gardes-Albert, *Methods Enzymol.*, **234**, 462 (1994); [https://doi.org/10.1016/0076-6879\(94\)34117-6](https://doi.org/10.1016/0076-6879(94)34117-6)
27. Y. Çetinkaya, H. Göçer, A. Menzek and I. Gülçin, *Arch. Pharm.*, **345**, 323 (2012); <https://doi.org/10.1002/ardp.201100272>
28. A. Venkanna, B. Siva, B. Poornima, P.R. Rao Vadaparathi, K.R. Prasad, K.A. Reddy, G.B.P. Reddy and K.S. Babu, *Fitoterapia*, **95**, 102 (2014); <https://doi.org/10.1016/j.fitote.2014.03.003>
29. S.J. Nadaf, N.R. Jadhav, H.S. Naikwadi, P.L. Savekar, I.D. Sapkal, M.M. Kambli and I.A. Desai, *OpenNano*, **8**, 100076 (2022); <https://doi.org/10.1016/j.onano.2022.100076>